学位論文

Heterogeneous expression and role of receptor tyrosine kinase-like orphan receptor 2 (ROR2) in small cell lung cancer
（小細胞肺癌における receptor tyrosine kinase-like orphan receptor 2（ROR2）の ヘテロ発現とその役割）

眞田　宗

Mune Sanada

熊本大学大学院医学教育部博士課程医学専攻呼吸器外科学

指導教員

鈴木　実　教授

熊本大学大学院医学教育部博士課程医学専攻呼吸器外科学

2023 年 3 月

学　位　論　文

論文題名　：　Heterogeneous expression and role of receptor tyrosine kinase-like orphan receptor 2 (ROR2) in small cell lung cancer
（小細胞肺癌における receptor tyrosine kinase-like orphan receptor 2（ROR2）の
ヘテロ発現とその役割）

著 者 名　：　眞田　宗
Mune　Sanada

指導教員名　：　熊本大学大学院医学教育部博士課程医学専攻呼吸器外科学　鈴木　実　教授

審査委員名　：　呼吸器内科学担当教授　　坂上　拓郎　教授

歯科口腔外科学担当教授　　中山　秀樹　教授

細胞医学担当教授　　中尾　光善　教授

小児外科学・移植外科学担当准教授　　菅原　寧彦　准教授

2023年3月

Original Article

Title:

Heterogeneous expression and role of receptor tyrosine kinase-like orphan receptor 2 (ROR2) in small cell lung cancer

Authors:

Mune Sanada[1,2], Masaya Yamazaki[3], Tatsuya Yamada[1], Kosuke Fujino[1], Shinji Kudoh[2], Yuki Tenjin[4], Haruki Saito[5], Noritaka Kudo[2,6], Younosuke Sato[2], Akira Matsuo[2,7], Makoto Suzuki[1], Takaaki Ito[2,7,8]

Affiliations:

[1] Department of Thoracic Surgery, Graduate School of Medical Science, Kumamoto University, 1-1-1 Honjo, Chuo-ku, Kumamoto 860-8556, Japan

[2] Department of Pathology and Experimental Medicine, Graduate School of Medical Science, Kumamoto University, 1-1-1 Honjo, Chuo-ku, Kumamoto 860-8556, Japan

[3] Department of Medical Biochemistry, Graduate School of Medical Science, Kumamoto University, 1-1-1 Honjo, Chuo-ku, Kumamoto 860-8556, Japan

[4] Department of Respiratory Medicine, Graduate School of Medical Science, Kumamoto University, 1-1-1

Honjo, Chuo-ku, Kumamoto 860-8556, Japan

[5] Departments of Otolaryngology-Head and Neck Surgery, Graduate School of Medical Science, Kumamoto University, 1-1-1 Honjo, Chuo-ku, Kumamoto 860-8556, Japan

[6] Department of Pathology, The University of Tokyo, 7–3–1 Hongo, Bunkyo-ku, Tokyo 113–0033, Japan.

[7] Department of Brain Morphology, Institute of Molecular Embryology and Genetics, Kumamoto University, 2-2-1 Honjo, Chuo-ku, Kumamoto 860-0811, Japan

[8] Department of Medical Technology, Faculty of Health Sciences, Kumamoto Health Science University, 325 Izumi, Kita-ku, Kumamoto, Kumamoto 861-5598, Japan

Corresponding author:

Takaaki Ito, M.D., D.M.Sci., Department of Pathology and Experimental Medicine, Kumamoto University, Graduate School of Medical Sciences, Honjo 1-1-1, Chuo-ku, Kumamoto 860-8556, Japan, Department of Brain Morphology, Institute of Molecular Embryology and Genetics, Kumamoto University, Honjo 2-2-1, Chuo-ku, Kumamoto 860-0811, Japan and Department of Medical Technology, Faculty of Health Science, Kumamoto Health Science University, 325 Izumi, Kita-ku, Kumamoto 861-5598, Japan. itou-ta@kumamoto-hsu.ac.jp

16-digit ORCID of the authors:

Masaya Yamazaki 0000-0003-4151-4983

Haruki Saito 0000-0001-9610-0951

Noritaka Kudo 0000-0002-6064-9149

Takaaki Ito 0000-0001-5528-3464

Acknowledgments:

We thank Ms. Takako Maeda and Ms. Yuko Fukuchi for their technical assistance, the staff of LILA for their technical support, and the Institute of Molecular Embryology and Genetics, Kumamoto University for its help with RNA sequencing and proteomics analyses.

Abstract:

The present study investigated the expression and role of ROR2 in small cell lung cancer (SCLC). To examine the expression of ROR2, 27 surgically resected SCLC tissue samples were immunostained for ROR2. Sixteen tissue samples were positive and some showed intratumor heterogeneity in staining intensity. The heterogeneity of ROR2 expression was also observed in tumor tissues from a PDX model of SCLC, in which there were cells with high ROR2 expression ($ROR2^{high}$ cells) and without its expression ($ROR2^{low}$ cells). These cells were subjected to a RNA sequence analysis. GSEA was performed and the results obtained revealed the enrichment of molecules such as G2M checkpoint, mitotic spindle, and E2F targets in $ROR2^{high}$ cells. The rate of EdU incorporation was significantly higher in $ROR2^{high}$ cells than $ROR2^{low}$ cells from the PDX model and the SCLC cell lines. Cell proliferation was suppressed in *ROR2* KO SBC3 cells *in vitro* and *in vivo*. Comparisons of down-regulated differentially expressed genes in *ROR2* KO SBC3 cells with up-regulated DEG in $ROR2^{high}$ cells from the PDX model revealed 135 common genes. After a Metascape analysis of these genes, we focused on Aurora kinases. In SCLC cell lines, the knockdown of ROR2 suppressed Aurora kinases. Therefore, ROR2 appears to regulate the cell cycle through Aurora kinases. The present results reveal a role for ROR2 in SCLC and afford a candidate system (ROR2-Aurora kinase) accompanying tumor heterogeneity in SCLC.

Keywords:

Aurora kinases; Cell proliferation; Heterogeneity; ROR2; Small cell lung cancer

1. Introduction

Lung cancer is one of the most lethal cancers worldwide. Small cell lung cancer (SCLC) accounts for 10-15% of all lung cancers and is characterized by rapid proliferation, high metastatic potential, high sensitivity to radiotherapy and chemotherapy, and the early acquisition of resistance to treatment [1,2]. In recent years, targeted therapies have been shown to reduce mortality in patients with non-small cell lung cancer (NSCLC), but marked improvements in the survival of patients with SCLC have not yet been achieved [3]. Therapeutic strategies with novel agents, such as immune checkpoint inhibitors, are being investigated; however, their long-term efficacy is unclear and therapeutic advances for SCLC are currently insufficient [3].

Receptor tyrosine kinase-like orphan receptor (ROR) belongs to the receptor tyrosine kinase family. ROR is a single-pass transmembrane receptor, the extracellular portion of which contains immunoglobulin-like, cysteine-rich, and kringle domains [4]. The cysteine-rich domain of ROR is essential for binding WNT ligands and transduces the WNT signaling pathway [5,6].

ROR expression has been reported in many cancers. In NSCLC, ROR1 has been identified as a transcriptional target of Nkx-2.1 and is highly expressed, particularly in lung adenocarcinomas [7]. A previous study reported that the suppression of ROR1 inhibited cell growth in epidermal growth factor receptor tyrosine kinase inhibitor (EGFR-TKI)-resistant cell lines, making it a promising therapeutic approach for EGFR-TKI-resistant lung cancer [8]. ROR2 expression in NSCLC was identified by

immunohistochemistry (IHC) in approximately 50% of cases, and its expression correlated with poor overall survival [9]. Correlations were also reported between high ROR expression and poor survival rates in pancreatic, breast, and cervical cancers [10.11.12]. On the other hand, in hepatocellular carcinoma, patients with low ROR2 expression had a poorer prognosis than those with high ROR2 expression [13]. High ROR2 expression in endometrial carcinoma has been associated with a good prognosis [14]. There are conflicting findings on the function of ROR2. In breast cancer, the knockdown of ROR2 suppressed cell proliferation, whereas its overexpression exerted the opposite effects [11]. In melanoma, ROR2 expression inhibited cell proliferation [15]. In colorectal cancer cell lines, the knockdown of ROR2 increased cellular proliferation and migration and decreased invasion [16], whereas it promoted cell migration and invasion in endometrial cancer [14].

Collectively, these findings suggest that ROR2 functions vary by origin and the histological type of cancer. However, ROR2 expression patterns and its biological roles in SCLC remain unclear. The transfection of Achaete scute complex homologue 1 (ASCL1) gene, a cell lineage-specific oncogene of SCLC [1], induced neuroendocrine differentiation in lung adenocarcinoma cell lines [17,18,19,20], and modulated WNT-related molecules, including WNT11 and ROR2, in an adenocarcinoma cell line [17,21]. WNT11 is important in the neuroendocrine differentiation and epithelial-mesenchymal transition of SCLC [17]; however, the significance of ROR2 in SCLC remains unknown.

In the present study, we attempted to clarify the role of ROR2 in SCLC. To confirm the

expression of ROR2, we performed IHC on surgically resected SCLC tissue samples and a flow cytometric analysis of a patient-derived xenograft (PDX) model. To focus on differences between $ROR2^{high}$ and $ROR2^{low}$ cells in the PDX model, we sorted cells by flow cytometry and performed a comprehensive analysis using RNA sequencing. We performed the knockdown and knockout of *ROR2* in SCLC cell lines to elucidate the molecular and biological functions of ROR2. We herein report on the expression and function of ROR2 in SCLC, including a comprehensive analysis.

2. Materials and Methods

2.1 Cell lines

Six SCLC cell lines (H69, H889, SBC1, H69AR, SBC3, and SBC5) were used in the present study. H69, H889, and H69AR were purchased from ATCC (Manassas, VA), and SBC1, SBC3, and SBC5 were from the Japan Collection of Research Bioresources Cell Bank (Osaka, Japan). All growth media were purchased from Wako Pure Chemical Industries (Osaka, Japan) and supplied with 1% penicillin/streptomycin (Sigma–Aldrich). H69 and H889 cells were grown in RPMI 1640 medium supplemented with 2 mM L-glutamine, 10 nM HEPES, 1 mM sodium pyruvate, 4.5 g/L glucose, 1.5 g/L sodium bicarbonate, and 10% fetal bobbin serum (FBS; 175012, NICHIREI BIOSCIENCES, Tokyo, Japan). H69AR cells were grown in RPMI 1640 medium supplemented with 20% FBS. SBC1 cells were grown in RPMI 1640 medium supplemented with 15% FBS. SBC3 and SBC5 cells were grown in EMEM with 10%

FBS. All cells were incubated at 37℃ in 5% CO_2 and saturated humidity. Cells were maintained as subconfluent cultures before use and harvested with trypsin-EDTA (Invitrogen, CA, USA).

2.2 Tissue Samples

Tissue samples of SCLC (n = 27) resected at the Department of Thoracic Surgery of Kumamoto University Hospital (Kumamoto, Japan) were used in the present study. Samples were histologically diagnosed according to the WHO criteria. These sections were used for IHC. The present study followed the guidelines of the Ethics Committee of Kumamoto University.

2.3 PDX model

The PDX model was created at the Departments of Thoracic Surgery and Pathology and Experimental Medicine, Kumamoto University. Surgical SCLC tissues were subcutaneously transplanted into the backs of immunodeficient mice (Rag2-/-:Jak3-/- mice; a generous gift from Prof. Seiji Okada [22]), and used in experiments after several passages. In the flow cytometric analysis, PDX tumor tissues were harvested when they had grown to a diameter of approximately 1 cm. They were then dissociated into 1-mm pieces and treated with TrypLE (Thermo Fisher, Waltham, MA) to make single cells. The present study followed the guidelines of the Ethics Committee of Kumamoto University. All animal experiments were conducted in accordance with the guidelines of the Animal Care and Use Committee of Kumamoto

University.

2.4 IHC

Formalin-fixed, paraffin-embedded specimens were cut into 3-μm-thick sections and mounted onto MAS-GP-coated slides (Matsunami Glass, Osaka, Japan). After deparaffinization and rehydration, sections were heated using an autoclave in 0.01 mol/L citrate buffer (pH 7.0) for antigen retrieval. Sections were incubated with 0.3% H_2O_2 in absolute methanol for 20 minutes to block endogenous peroxidase activity. Sections were incubated with skimmed milk for 30 minutes to block non-specific staining. After this blocking step, sections were incubated with the primary antibodies (Table 1) at 4°C overnight, followed by sequential 1-hour incubations with the secondary antibodies (En Vision+System-HRP-Labeled polymer; K4001, K4003, Dako, Santa Clara, CA) and visualization with the liquid DAB+substrate Chromogen System (K3468, Dako). All slides were counterstained with hematoxylin for 30 seconds before being dehydrated and mounted. Areas stained using IHC were scored according to a 4-tier system: no staining area, positive staining area <10% SCLC tumor cells stained, positive staining area 10–50% SCLC tumor cells stained, and positive staining area > 50% SCLC tumor cells stained. Scoring was simultaneously performed by two independent researchers (M.S. and T.I.) who were blinded to patient details.

2.5 Western blot (WB) analysis

Cells were prepared for a WB analysis as previously reported [23]. A list of the primary antibodies used is shown in Table 1. The membrane was incubated with the primary antibodies at 4℃ overnight. The membrane was then washed and incubated with the respective secondary antibodies conjugated with horseradish peroxidase (7074S, 7076S, Cell Signaling, Danvers, MA) at room temperature for 1 hour, and the immune complex was visualized with chemiluminescence substrate ECL prime (RPN2236, Amersham Pharmacia Biotech, Amersham, UK).

2.6 *ROR2* KO vector plasmid construction and transfection

Genome editing using CRISPR/ Cas9 was used to KO the ROR2 gene in the SBC3 cell line. pSpCas9(BB)-2A-Puro(px459) was purchased from Addgene (Cambridge, MA). The sgRNA target sequences of *ROR2* were as follows: TGC TGT GCA TCC CGG CCG TC. These plasmids were co-transfected with Lipofectamine 3000 (L3000-015, Thermo Fisher Scientific) into cells at subconfluency. After 48 hours, transfected cells were treated with 1 μg/mL puromycin (Clontech Laboratories, Mountain View, CA) for the selection of stably transfected cells.

2.7 Transfection with siRNA

si*ROR2* (Cat#: 4390824) and Silencer Negative Control siRNA#1 (Cat#: AM4611) were purchased from Ambion (Austin, TX, USA). H69 cells were transfected with siRNA at a concentration of

30 nmol/L using an electroporator (NEPA21 pulse generator; Nepa Gene, Chiba, Japan). SBC3 and SBC5 cells were transfected with siRNA at a concentration of 30 nmol/L using Lipofectamine RNAiMAX (13778-150, Thermo Fisher Scientific). Cells were harvested 48 hours post-transfection.

2.8 Tumor xenograft growth and histopathological evaluation

A total of 1.0×10^6 cells each of mock SBC3 cells and *ROR2* KO SBC3 cells (mixture of the three clones in equal proportions) were subcutaneously injected into the backs of Rag2-/-:Jak3-/- mice. Twenty-eight days after the injection, tumors were removed and measured. Samples were fixed with phosphate-buffered 4 % paraformaldehyde solution and embedded in paraffin. Tissue sections were stained with hematoxylin and eosin, and additional sections were used for an immunohistochemical analysis.

2.9 Cell counting assay

Mock SBC3 cells and *ROR2* KO SBC3 cells were seeded at equivalent densities (2.0×10^5 cells/well) in 6-well plates. After 24, 48, 72, 96, 120, and 144 hours, cells were trypsinized and counted. Experiments were repeated in triplicate to confirm reproducibility.

2.10 Flow cytometry

Tumor cells were suspended in FACS buffer (PBS(-) with 0.1% NaN_3, 2% FBS) or sorting buffer

(PBS(-) with 2% FBS, 1 mM EDTA, and 25 mM HEPES). Cells were stained with antibodies against human ROR2 (APC-conjugated, FAB20641A, 1:10, R&D SYSTEMS, Minneapolis, MN), mouse H-2Kd/H-2Dd (PE/Cy7-conjugated, 114718, 1:100, BioLegend, San Diego, CA), or a mouse IgG2a isotype control (APC-conjugated, IC003A, 1:10, R&D SYSTEMS) on ice for 30 minutes in the dark. After washing, cells were resuspended in FACS buffer or sorting buffer with 7-AAD (420404, 1:100, BioLegend) to stain dead cells. A flow cytometric analysis was performed using FACSVerse (BD Biosciences, Franklin Lakes, NJ) or FACS Aria III (BD Biosciences).

2.11 5-Ethynyl-2'-deoxyuridine (EdU) incorporation

Regarding the EdU labeling of cells (H69, SBC3, and SBC5), each cell was incubated with a final concentration of 10 μM EdU (C10632, Invitrogen) at 37℃ for 3 hours. EdU (052-08843, FUJIFILM, Tokyo, Japan) dissolved in PBS was administered to PDX mice via an intraperitoneal injection (1 mg/each). Tumors were harvested 3 hours after the EdU injection. The incorporation of EdU was detected using the Click-iTTM Plus EdU Alexa FluorTM 488 Flow Cytometry Assay Kit (C10632, Invitrogen) according to the manufacturer's instructions. Dead cells were stained using the LIVE⁄DEAD Fixable Dead Cell Stain Kit (L34963, 1:1000, Thermo Fisher). All samples were analyzed using FACSVerse.

2.12 RNA sequence analysis

Regarding *ROR2* KO SBC3 cells, total RNA was extracted from cultured cells using a RNeasy Mini Kit (Cat.74134, Qiagen, Hilden, Germany). A 2100 Bioanalyzer (Agilent, Santa Clara, CA) was used to detect the concentration and purity of total RNA. All samples with an RNA integrity number >7.5 were used for sequencing. The RNA-seq library was prepared using a TruSeq Stranded mRNA Library Prep Kit (20020594, Illumina, San Diego, CA) and sequenced using NextSeq 500 (Illumina).

Concerning the PDX model, $ROR2^{high}$ and $ROR2^{low}$ cells were sorted using FACS Aria III (BD Biosciences) and directly collected into CDS Sorting Solution (contained in the SMART-seq HT kit). cDNA was then synthesized without RNA purification using SMART-seq HT (634455, Takara, Shiga, Japan). The RNA-seq library was prepared using a Nextera XT Library Prep Kit (FC-131-1024, FC-131-1001, Illumina) and sequenced using the Hiseq X Ten sequencer (Illumina).

RNA-seq reads were aligned to a human transcriptome (GRCh38) and quantified by Salmon [24] (version 1.3.0) with default settings. Differential expression testing was performed with DESeq2 (version 1.28.1). A p-value threshold of <0.05 was used to identify differentially expressed genes (DEG). A Metascape (https://metascape.org) analysis was performed with hallmark gene sets and canonical pathways. A GSEA (version 4.1.0) (Broad Institute) analysis was performed with hallmark gene sets and PID gene sets.

2.13 Statistical analysis

All data were obtained from independent experiments and expressed as the means ±SD of triplicate measurements. Differences in mean values between the two groups were statistically analyzed using the *t*-test. Prism v.7 software (GraphPad Software, San Diego, CA) was used for statistical analyses. $p < 0.05$ was considered to be significant.

2.14 Data availability

The accession number for RNA sequence data in the present study is GEO: GSE 210388

3. Results

3.1 ROR2 expression in SCLC tissues and cell lines

To investigate the expression of ROR2, 27 surgically resected SCLC tissue samples were stained by IHC for ROR2. ROR2 positively stained in the cell membrane and cytoplasm (Fig. 1A). Sixteen tissue samples were positive for ROR2 and some of the stained tissues showed intratumor heterogeneity in staining intensity (Fig. 1B). A WB analysis of SCLC cell lines was performed, and ROR2 expression was observed in three out of the six SCLC cell lines tested (Fig. 1C).

3.2. Intratumor heterogeneity of ROR2 expression in the SCLC PDX model

To investigate the intratumor heterogeneity of ROR2 expression, a flow cytometric analysis was

applied to the PDX model. Four PDX models were established and analyzed with IHC (data not shown). A PDX model in which the intratumor heterogeneity of ROR2 was observed by IHC (Fig. 2A) was used for a flow cytometric analysis. The results of the flow cytometric analysis showed heterogeneity in ROR2 expression similar to those of IHC (Fig. 2B). To assess differences in gene expression patterns, $ROR2^{high}$ and $ROR2^{low}$ cells were sorted by flow cytometry (Fig. 2B) and a RNA sequence analysis of $ROR2^{high}$ and $ROR2^{low}$ cells was performed. A heatmap shows differences in gene expression patterns between $ROR2^{high}$ and $ROR2^{low}$ cells (Fig. 2C). A total of 1790 genes were identified as DEG (p value <0.05). Overall, 999 genes were up-regulated in $ROR2^{high}$ cells and 791 in $ROR2^{low}$ cells. GSEA was performed and the results obtained revealed the enrichment of HALLMARK_G2M_CHECKPOINT, HALLMARK_MITOTIC_SPINDLE, and HALLMARK_E2F_TARGETS in $ROR2^{high}$ cells (Fig. 2D,2E,Supplymental file1). Expressions of CyclinB1, CyclinB2 and CDK1 are upregulated in $ROR2^{high}$ cells (Fig. 2F). These results suggest a role for ROR2 in cell division.

3.3. Increased EdU incorporation in $ROR2^{high}$ cells

The results of the RNA sequence analysis suggested that the cell cycle is enhanced in $ROR2^{high}$ cells. To confirm this, we evaluated the incorporation of EdU in PDX cells. The heterogeneity of ROR2 expression was confirmed by a flow cytometric analysis, and the rate of EdU incorporation was significantly higher in $ROR2^{high}$ cells than in $ROR2^{low}$ cells (Fig. 3A). Similar analyses were performed

using ROR2-positive SCLC cell lines (Fig. 1C). A flow cytometric analysis of the H69, SBC3, and SBC5 cell lines showed heterogeneity in the expression of ROR2 (Fig. 3B, C, D). These cell lines were evaluated for the incorporation of EdU using flow cytometry. In the H69, SBC3, and SBC5 cell lines, EdU incorporation rates were higher in $ROR2^{high}$ cells than in $ROR2^{low}$ cells (Fig. 3B, C, D). These results indicated an enhanced cell cycle of $ROR2^{high}$ cells in SCLC.

3.4. Suppressed proliferation of ROR2 KO SBC3 cells

To investigate the function of ROR2, the ROR2 gene was KO in SBC3 cells using CRISPR/Cas9. ROR2 was not detected in *ROR2* KO SBC3 cells by a WB analysis (Fig. 4A). Cell proliferation under culture conditions was significantly lower in *ROR2* KO SBC3 cells than in mock SBC3 cells (Fig. 4B). Mock and *ROR2* KO SBC3 cells were subcutaneously injected into the backs of immunocompromised mice. The tumors arising in the back were removed and measured 28 days after the inoculation. The size and weight of xenotransplanted tumors from *ROR2* KO SBC3 cells were slightly smaller than those from mock SBC3 cells (Fig. 4 C, D). Xenotransplanted tumors were histologically similar, regardless of the ROR2 expression status, whereas ROR2 was not immunohistochemically detected in the tumors from *ROR2* KO cells (Fig. 4E).

3.5. Search for ROR2-related molecules

A RNA sequence analysis was performed for mock and *ROR2* KO SBC3 cells, and DEG was evaluated. In total, 1738 genes were down-regulated in *ROR2* KO SBC3 cells. Comparisons of down-regulated DEG in *ROR2* KO SBC3 cells and up-regulated DEG in ROR2^{high} cells revealed 135 common genes (Fig. 5A). These 135 genes were analyzed using Metascape, and those involved in the cell cycle, such as HALLMARK_E2F_TARGETS and HALLMARK_G2M_CHECKPOINT, were enriched (Fig. 5B). PID AURORA B PATHWAY was enriched as a pathway, and the genes included in the PID AURORA B PATHWAY and PID AURORA A PATHWAY were indicated (Fig. 5A). Since we speculated that the expression of ROR2 may in turn affect the expression of AURKA and AURKB, we performed the knockdown of ROR2 in the H69, SBC3, and SBC5 cell lines, and a WB analysis revealed that the expression of AURKA, AURKB and Phospho-Histone H3 was decreased in these cells (Fig. 5C). These results suggest that ROR2 affected the cell cycle through the expression of AURKA and/or AURKB.

4. Discussion

ROR2 is up-regulated in various carcinomas and is considered to be involved in cell proliferation, EMT, and other biological properties, suggesting its potential as a therapeutic target for cancer [25]. In SCLC, ROR2 has been identified as a molecular target of ASCL1 and SOX2, critical transcription factors of SCLC [17,21,26], has been less focused than ROR1 in lung adenocarcinoma [7]. Through our IHC studies on surgically resected samples and PDX models of SCLC, WB of SCLC cell lines, and flow

cytometric analyses of PDX model cells and cell lines, it has become evident that ROR2 is expressed with inter- and intra-tumor heterogeneities in SCLC.

Tumor heterogeneity involves aggressive tumor characteristics, such as frequent metastasis and resistance to treatments [27], and this also appears to be the case in SCLC [28]. In addition, although SCLC has been treated as a homogeneous tumor based on its genetic and biological backgrounds, comprehensive analyses have revealed differences in gene expression patterns and drug sensitivity [29,30]. A PDX model for SCLC has been reported to accurately recapitulate the pathological morphology, genomic alterations, and expression profiles of clinical specimens as SCLC, and is considered to be more similar to the clinical model of SCLC [31,32]. In the present study, we used the PDX model to analyze the role of ROR2. A comprehensive RNA-seq analysis of differences between ROR2^{high} and ROR2^{low} cells in the PDX model revealed the enrichment of genes related to the cell cycle. Therefore, we hypothesized that ROR2 is involved in cell proliferation, which is supported by the greater incorporation of EdU in PDX ROR2^{high} cells than in ROR2^{low} cells. Moreover, cell proliferation was suppressed in *ROR2* KO SBC3 cells.

We searched for ROR2-associated molecules using a differential analysis of ROR2-expressing cells and a comprehensive RNA-seq analysis of *ROR2* KO SBC3 cell lines and focused on Aurora kinases. Aurora kinases are a group of serine-threonine kinases that play an important role in mitosis [33]. They are up-regulated in many carcinomas and correlate with the prognosis of patients, which make them a potential target for cancer therapy [34]. A phase II trial on the treatment of SCLC with an Aurora kinase A inhibitor

(Alisertib) is currently underway [35]. In the present study, Aurora kinases were up-regulated in PDX ROR2^{high} cells and down-regulated in the three SCLC cell lines with the knockdown of *ROR2*. These results indicate that ROR2 regulates the expression of Aurora kinase, which may be involved in the cell cycle and activation of cell proliferation. Forkhead box M1 (FOXM1) has been identified as an upstream molecule that regulates Aurora kinases [34,36]. Our comprehensive analysis also identified the FOXM1 pathway, suggesting that ROR2 regulates Aurora kinases via FOXM1; however, the underlying mechanisms remain unknown. The therapeutic efficacy of Aurora kinase inhibitors in SCLC was previously reported to be higher for NEUROD1/MYC-expressing SCLC [30], and alisertib/paclitaxel have been shown to prolong progression-free survival in patients with MYC-expressing SCLC [35]. An analysis of a dataset [37] revealed that ROR2 expression positively correlated with NEUDO1; therefore, controlling a subset of SCLC with the ROR2-NEUROD1-Aurorakinase system is a future direction for research on SCLC.

The identification of ligands is important for elucidating the molecular mechanisms underlying the ROR2 signaling pathway. ROR2 is considered to be a receptor for WNT because it has a CRD similar to FZD [25]. We previously reported the increased expression of WNT11 and its involvement in cell proliferation, EMT, and cell growth in SCLC and ASCL1-induced neuroendocrine carcinoma [17]. In breast cancer, WNT11 has also been shown to act with the CRD of ROR2 in order to enhance cell invasion [38]. Since the knockdown of *WNT11* and KO of *ROR2* both inhibited cell proliferation in SCLC cell lines, WNT11 may be a candidate ligand for ROR2 in SCLC. However, WNT11 does not appear to be a ligand

for ROR2 because the SBC3 cell line, in which the proliferation of *ROR2* KO cells was reduced, does not express WNT11 and recombinant human WNT11 does not modify Wnt signaling in ROR2-positive SCLC cells (unpublished observations). Therefore, there may be ligands other than WNT11 for ROR2 in SCLC cells.

In summary, we herein demonstrated that ROR2 was heterogeneously expressed in SCLC and played an important role in cell proliferation. A comprehensive RNA-seq analysis of ROR2 identified Aurora kinases as ROR2-associated molecules. These results suggest that Aurora kinases are involved in the regulation of cell proliferation by ROR2. The present results provide a more detailed understanding of the significance of ROR2 in SCLC and will contribute to the development of new treatments for SCLC and improvements in the prognosis of patients.

Declarations

Funding: The present study was supported in part by the program of the Joint Usage/Research Center for Developmental Medicine, Institute of Molecular Embryology and Genetics, Kumamoto University, by a Grant-in-Aid for Scientific Research from the Ministry of Education, Culture, Sports, Science and Technology of Japan (20H03691), by a Grant from the Smoking Research Foundation, and by endowments from Dr. Yukoh Aihara of Aihara Allergy and Pediatric Clinic and from Prof. Kimitaka Itoh, Chubu University.

Conflicts of interest: The authors have no conflicts of interest to declare.

Ethical approval: All studies using human pathological samples and surgically resected tissues followed the guidelines of the Ethics Committee of Kumamoto University (No. 342 and genome No. 423). All animal experiments were conducted in accordance with the guidelines of the Animal Care and Use Committee of Kumamoto University (No. 2021-034).

Figure legends

Fig. 1. Expression of ROR2 in small cell lung cancer (SCLC). **A.** Immunohistochemical staining of ROR2 in surgically resected SCLC tissues. **B.** Proportion of each positive staining areas for ROR2 in SCLC tissue samples. **C.** Western blotting analysis of 6 SCLC cell lines for ROR2 and ROR1.

Fig. 2. Difference between $ROR2^{low}$ cells and $ROR2^{high}$ cells in the PDX model. **A**. Immunohistochemical staining of ROR2 in the PDX model. **B**. FACS gating for sorting $ROR2^{low}$ and $ROR2^{high}$ cells. Mouse cells expressing H-2Kd/H-2Dd were eliminated. **C**. Heatmap of differentially expressed genes (DEG) in $ROR2^{low}$ and $ROR2^{high}$ cells in the PDX model. **D**. Gene Set Enrichment Analysis (GSEA) comparing $ROR2^{low}$ and $ROR2^{high}$ cells (FDR <0.25) in the PDX model. **E**. Three significant gene sets related to cell division (or proliferation) (arrows in Fig. 2D) are extracted and displayed. F. Transcripts per million (TPM) of CyclinB1, CyclinB2 and CDK1 are upregulated in $ROR2^{high}$ cells, compared to $ROR2^{low}$ cells. Data are presented as means ± SD. *$p < 0.05$. **$p < 0.01$.

Fig. 3. The incorporation of 5-ethynyl-2'-deoxyuridine (EdU) by SCLC. **A**. PDX model, **B**. H69 cell line, **C**. SBC3 cell line, **D**. SBC5 cell line. $ROR2^{low}$ and $ROR2^{high}$ sorting gates are shown. EdU-positive cells in $ROR2^{low}$ cells and $ROR2^{high}$ cells are shown. Experiments were repeated in triplicate to confirm

reproducibility. One example of flow cytometry data from each cell is shown. Data are presented as means ± SD. **$p < 0.01$.

Fig. 4. Proliferation of *ROR2* KO SBC3 cell lines. **A.** WB analysis of *ROR2* KO SBC3 cell lines. **B.** Cell counting assay with *ROR2* KO SBC3 cell lines. **C.** Xenograft of mock and *ROR2* KO SBC3 cell lines. Scale bar = 10 mm. **D.** Weight comparison of tumors of mock and *ROR2* KO SBC3 cell xenografts. **E.** H&E and immunohistochemical staining of ROR2 in xenografted tumors. Data are presented as means ± SD. *$p < 0.05$. **$p < 0.01$.

Fig. 5. Search for ROR2-related molecules. **A.** Comparison of down-regulated DEG in *ROR2* KO SBC3 cell lines and up-regulated DEG in $ROR2^{high}$ cells of the PDX model. The genes included in the PID AURORA B PATHWAY and PID AURORA A PATHWAY are indicated in red. **B.** A Metascape analysis of 135 common genes. **C.** A WB analysis of AURKA, AURKB, and pHH3 in the H69, SBC3, and SBC5 cell lines with the knockdown of *ROR2*.

Table 1 List of antibodies

Primary antibody	Manufacturer	IHC	FCM	WB
ROR2 (MA5-27244)	Invitrogen	1:200		
ROR2 (FAB20641A)	R&D		1:10	
ROR2 (MABS1152)	Millipore			1:500
ROR1 (#4102)	Cell signaling			1:200

AURKA (A1231)	Sigma Aldrich	1:1000
AURKB (ab2254)	Abcam	1:1000
pHH3 (06-570)	Millipore	1:1000
β-actin (A-5441)	Sigma Aldrich	1:40000

Antibodies used for IHC, FCM, and WB. Product number, manufacturer, and working dilutions are indicated. ROR2 receptor tyrosine kinase-like orphan receptor 2, ROR1 receptor tyrosine kinase-like orphan receptor 1, AURKA Aurora kinase A, AURKB Aurora kinase B, pHH3 Phospho-Histone H3

References

[1] Gazdar AF, Bunn PA, Minna JD. Small-cell lung cancer: what we know, what we need to know and the path forward. Nat Rev Cancer. 2017; 17:725-37.

[2] Rodriguez E, Lilenbaum RC. Small cell lung cancer: past, present, and future. Curr Oncol Rep. 2010; 12:327-34.

[3] Howlader N, Forjaz G, Mooradian MJ, et al. The effect of advances in lung-cancer treatment on population mortality. N Engl J Med. 2020; 383:640-49.

[4] Masiakowski P, Carroll RD. A novel family of cell surface receptors with tyrosine kinase-like domain. J Biol Chem. 1992; 267:26181-90.

[5] Xu YK, Nusse R. The Frizzled CRD domain is conserved in diverse proteins including several receptor tyrosine kinases. Curr Biol. England, 1998; R405-6.

[6] Masiakowski P, Yancopoulos GD. The Wnt receptor CRD domain is also found in MuSK and related orphan receptor tyrosine kinases. Curr Biol. England, 1998; R407.

[7] Yamaguchi T, Yanagisawa K, Sugiyama R, et al. NKX2-1/TITF1/TTF-1-Induced ROR1 is required to sustain EGFR survival signaling in lung adenocarcinoma. Cancer Cell. 2012; 21:348-61.

[8] Yamaguchi T, Lu C, Ida L, et al. ROR1 sustains caveolae and survival signalling as a scaffold of cavin-1 and caveolin-1. Nat Commun. 2016; 7:10060.

[9] Lu C, Wang X, Zhu H, Feng J, Ni S, Huang J. Over-expression of ROR2 and Wnt5a cooperatively correlates with unfavorable prognosis in patients with non-small cell lung cancer. Oncotarget. 2015; 6:24912-21.

[10] Huang J, Fan X, Wang X, et al. High ROR2 expression in tumor cells and stroma is correlated with poor prognosis in pancreatic ductal adenocarcinoma. Sci Rep. 2015; 5:12991..

[11] Guo M, Ma G, Zhang X, et al. ROR2 knockdown suppresses breast cancer growth through PI3K/ATK signaling. Aging (Albany NY). 2020; 12:13115-27.

[12] Sun B, Ye X, Lin L, Shen M, Jiang T. Up-regulation of ROR2 is associated with unfavorable prognosis

and tumor progression in cervical cancer. Int J Clin Exp Pathol. 2015; 8:856-61.

[13] Geng M, Cao YC, Chen YJ, Jiang H, Bi LQ, Liu XH. Loss of Wnt5a and Ror2 protein in hepatocellular carcinoma associated with poor prognosis. World J Gastroenterol. 2012; 18:1328-38.

[14] Henry CE, Llamosas E, Daniels B, Coopes A, Tang K, Ford CE. ROR1 and ROR2 play distinct and opposing roles in endometrial cancer. Gynecol Oncol. 2018; 148:576-84.

[15] Castro MV, Barbero GA, Villanueva MB, et al. ROR2 has a protective role in melanoma by inhibiting Akt activity, cell-cycle progression, and proliferation. J Biomed Sci. 2021; 28:76.

[16] Ma SS, Srivastava S, Llamosas E, et al. ROR2 is epigenetically inactivated in the early stages of colorectal neoplasia and is associated with proliferation and migration. BMC Cancer. 2016; 16:508.

[17] Tenjin Y, Kudoh S, Kubota S, et al. Ascl1-induced Wnt11 regulates neuroendocrine differentiation, cell proliferation, and E-cadherin expression in small-cell lung cancer and Wnt11 regulates small-cell lung cancer biology. Lab Invest. 2019; 99:1622-35.

[18] Osada H, Tomida S, Yatabe Y, et al. Roles of achaete-scute homologue 1 in DKK1 and E-cadherin repression and neuroendocrine differentiation in lung cancer. Cancer Res. 2008; 68:1647-55.

[19] Fujino K, Motooka Y, Hassan WA, et al. Insulinoma-associated protein 1 is a crucial regulator of neuroendocrine differentiation in lung cancer. Am J Pathol. 2015; 185:3164-77.

[20] Ito T, Kudoh S, Ichimura T, Fujino K, Hassan WA, Udaka N. Small cell lung cancer, an epithelial to mesenchymal transition (EMT)-like cancer: significance of inactive Notch signaling and expression of achaete-scute complex homologue 1. Hum Cell. 2017; 30:1-10.

[21] Kudoh S, Tenjin Y, Kameyama H, et al. Significance of achaete-scute complex homologue 1 (ASCL1) in pulmonary neuroendocrine carcinomas; RNA sequence analyses using small cell lung cancer cells and Ascl1-induced pulmonary neuroendocrine carcinoma cells. Histochem Cell Biol. 2020; 153:443-56.

[22] Ono A, Hattori S, Kariya R, et al. Comparative study of human hematopoietic cell engraftment into BALB/c and C57BL/6 strain of rag-2/jak3 double-deficient mice. J Biomed Biotechnol. 2011; 2011:539748.

[23] Yoshida R, Nagata M, Nakayama H, et al. The pathological significance of Notch1 in oral squamous

cell carcinoma. Lab Invest. 2013; 93:1068-81.

[24] Patro R, Duggal G, Love MI, Irizarry RA, Kingsford C. Salmon provides fast and bias-aware quantification of transcript expression. Nat Methods. 2017; 14:417-19.

[25] Menck K, Heinrichs S, Baden C, Bleckmann A. The WNT/ROR pathway in cancer: from signaling to therapeutic intervention. Cells. 2021; 10.

[26] Borromeo MD, Savage TK, Kollipara RK, et al. ASCL1 and NEUROD1 reveal heterogeneity in pulmonary neuroendocrine tumors and regulate distinct genetic programs. Cell Rep. 2016; 16:1259-72.

[27] Shibue T, Weinberg RA. EMT, CSCs, and drug resistance: the mechanistic link and clinical implications. Nat Rev Clin Oncol. 2017; 14:611-29.

[28] Lim JS, Ibaseta A, Fischer MM, et al. Intratumoural heterogeneity generated by Notch signalling promotes small-cell lung cancer. Nature. 2017; 545:360-64.

[29] Rudin CM, Poirier JT, Byers LA, et al. Molecular subtypes of small cell lung cancer: a synthesis of

human and mouse model data. Nat Rev Cancer. 2019; 19:289-97.

[30] Gay CM, Stewart CA, Park EM, et al. Patterns of transcription factor programs and immune pathway activation define four major subtypes of SCLC with distinct therapeutic vulnerabilities. Cancer Cell. 2021; 39:346-60.e7.

[31] Caeser R, Egger JV, Chavan S, et al. Genomic and transcriptomic analysis of a library of small cell lung cancer patient-derived xenografts. Nat Commun. 2022; 13:2144.

[32] Drapkin BJ, George J, Christensen CL, et al. Genomic and functional fidelity of small cell lung cancer patient-derived xenografts. Cancer Discov. 2018; 8:600-15.

[33] Glover DM, Leibowitz MH, McLean DA, Parry H. Mutations in aurora prevent centrosome separation leading to the formation of monopolar spindles. Cell. 1995; 81:95-105.

[34] Du R, Huang C, Liu K, Li X, Dong Z. Targeting AURKA in cancer: molecular mechanisms and opportunities for cancer therapy. Mol Cancer. 2021; 20:15.

[35] Owonikoko TK, Niu H, Nackaerts K, et al. Randomized phase II study of paclitaxel plus alisertib versus paclitaxel plus placebo as second-line therapy for SCLC: primary and correlative biomarker analyses. J Thorac Oncol. 2020; 15:274-87.

[36] Yang N, Wang C, Wang Z, et al. FOXM1 recruits nuclear Aurora kinase A to participate in a positive feedback loop essential for the self-renewal of breast cancer stem cells. Oncogene. 2017; 36:3428-40.36(24):3428–40.

[37] Jiang L, Huang J, Higgs BW, et al. Genomic landscape survey identifies SRSF1 as a key oncodriver in small cell lung cancer. PLoS Genet. 2016; 12:e1005895.

[38] Menck K, Heinrichs S, Wlochowitz D, et al. WNT11/ROR2 signaling is associated with tumor invasion and poor survival in breast cancer. J Exp Clin Cancer Res. 2021; 40:395.

Fig1

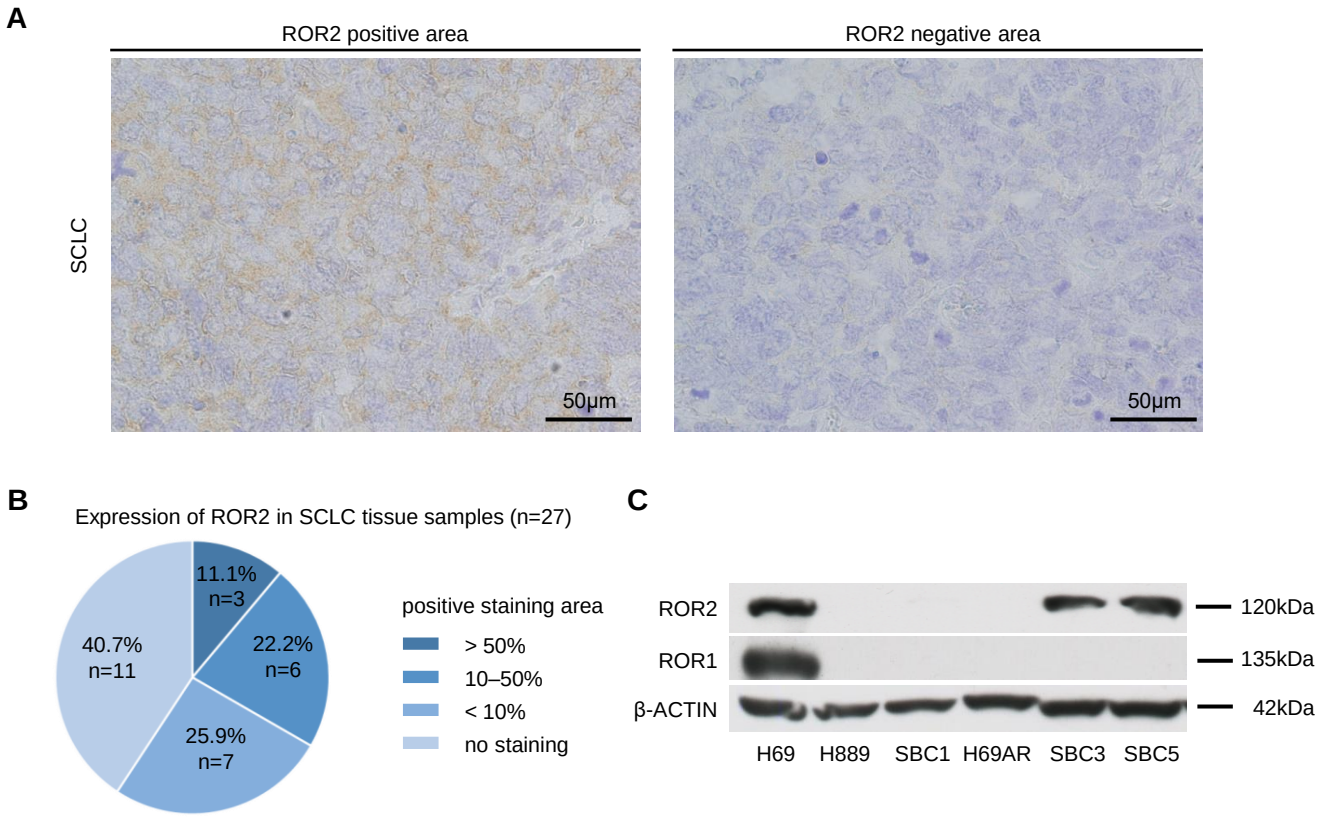
A
ROR2 positive area
ROR2 negative area
SCLC
50μm
50μm
B
Expression of ROR2 in SCLC tissue samples (n=27)
11.1%
n=3
22.2%
n=6
25.9%
n=7
40.7%
n=11
positive staining area
> 50%
10–50%
< 10%
no staining
C
ROR2
ROR1
β-ACTIN
120kDa
135kDa
42kDa
H69
H889
SBC1
H69AR
SBC3
SBC5

Fig2

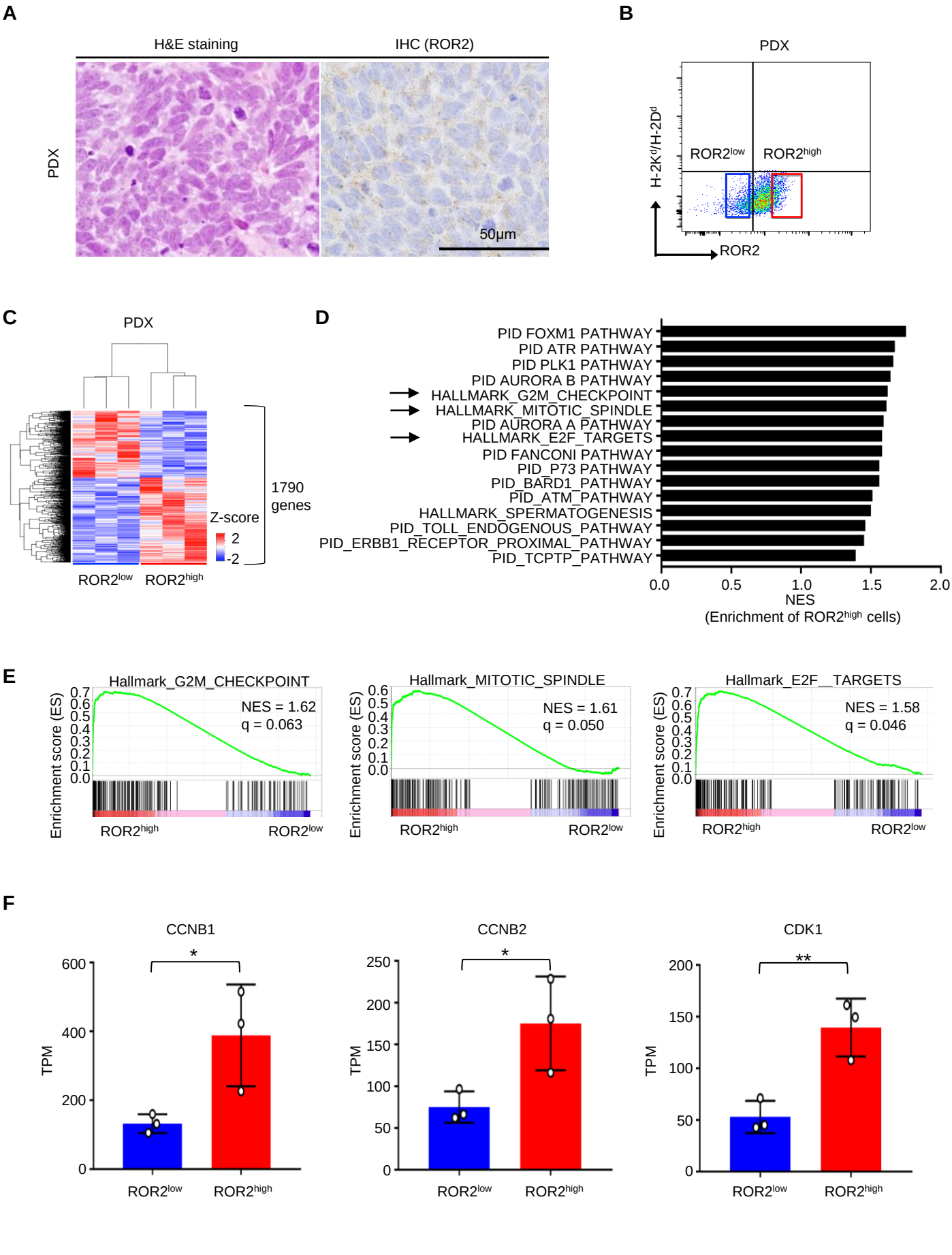
A
H&E staining
IHC (ROR2)
PDX
50μm
B
PDX
ROR2low
ROR2high
H-2Kd/H-2Dd
ROR2
C
PDX
1790 genes
Z-score
2
-2
ROR2low
ROR2high
D
PID FOXM1 PATHWAY
PID ATR PATHWAY
PID PLK1 PATHWAY
PID AURORA B PATHWAY
HALLMARK_G2M_CHECKPOINT
HALLMARK_MITOTIC_SPINDLE
PID AURORA A PATHWAY
HALLMARK_E2F_TARGETS
PID FANCONI PATHWAY
PID_P73 PATHWAY
PID_BARD1_PATHWAY
PID_ATM_PATHWAY
HALLMARK_SPERMATOGENESIS
PID_TOLL_ENDOGENOUS_PATHWAY
PID_ERBB1_RECEPTOR_PROXIMAL_PATHWAY
PID_TCPTP_PATHWAY
0.0
0.5
1.0
1.5
2.0
NES
(Enrichment of ROR2high cells)
E
Hallmark_G2M_CHECKPOINT
NES = 1.62
q = 0.063
Hallmark_MITOTIC_SPINDLE
NES = 1.61
q = 0.050
Hallmark_E2F__TARGETS
NES = 1.58
q = 0.046
Enrichment score (ES)
ROR2high
ROR2low
F
CCNB1
CCNB2
CDK1
TPM
*
**
ROR2low
ROR2high

Fig3

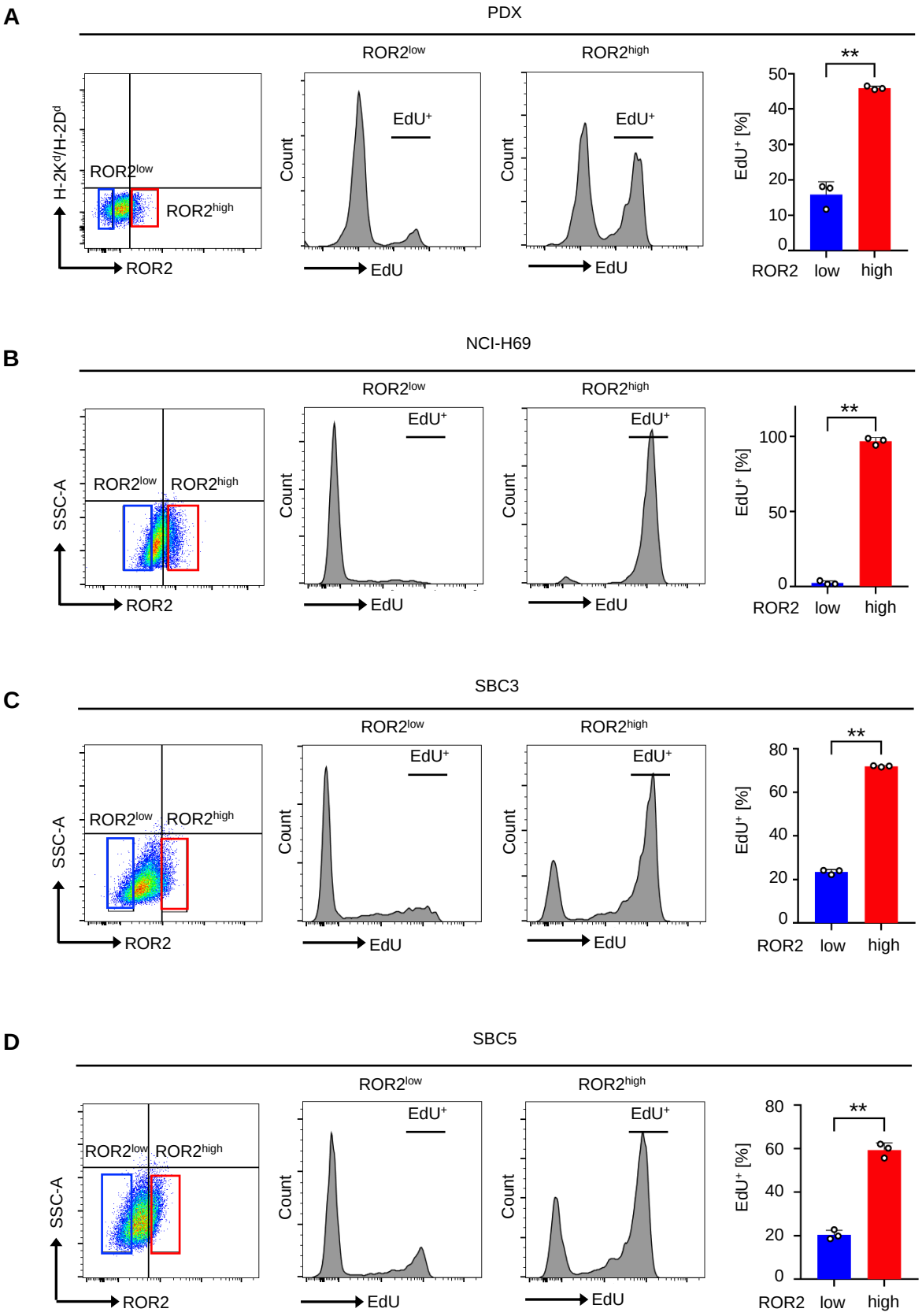
A
PDX
ROR2low
ROR2high
H-2Kd/H-2Dd
ROR2
Count
EdU+
EdU
EdU+ [%]
**
B
NCI-H69
SSC-A
C
SBC3
D
SBC5

Fig4

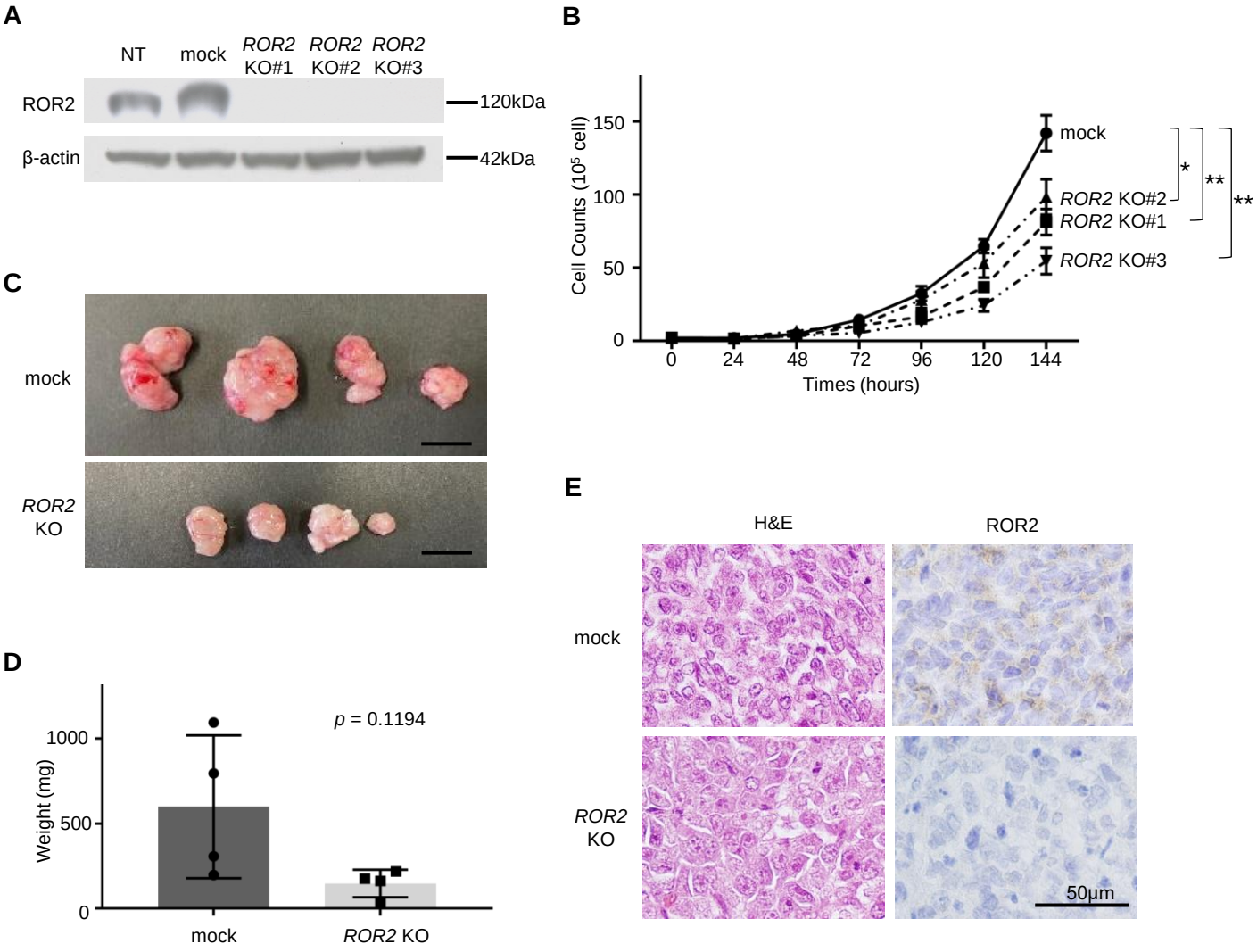
A
NT
mock
ROR2 KO#1
ROR2 KO#2
ROR2 KO#3
ROR2
120kDa
β-actin
42kDa
B
Cell Counts (10⁵ cell)
150
100
50
0
0
24
48
72
96
120
144
Times (hours)
mock
ROR2 KO#2
ROR2 KO#1
ROR2 KO#3
*
**
**
C
mock
ROR2 KO
D
Weight (mg)
1000
500
0
p = 0.1194
mock
ROR2 KO
E
H&E
ROR2
mock
ROR2 KO
50μm

Fig5

A

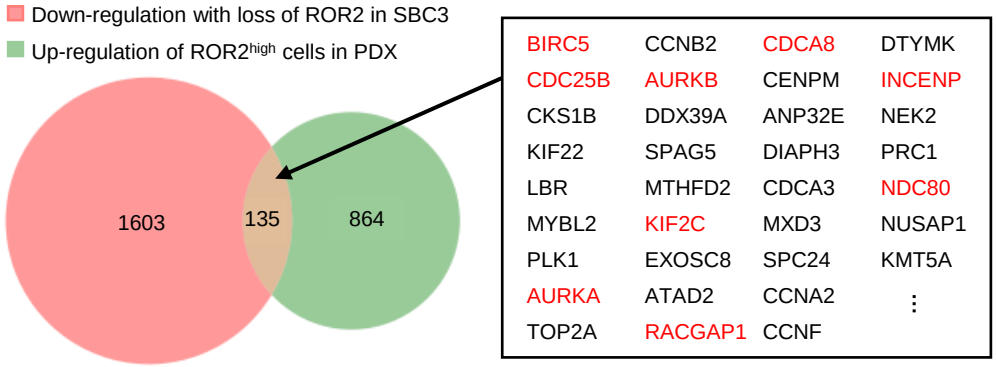
Down-regulation with loss of ROR2 in SBC3
Up-regulation of ROR2high cells in PDX
1603
135
864
BIRC5 CCNB2 CDCA8 DTYMK
CDC25B AURKB CENPM INCENP
CKS1B DDX39A ANP32E NEK2
KIF22 SPAG5 DIAPH3 PRC1
LBR MTHFD2 CDCA3 NDC80
MYBL2 KIF2C MXD3 NUSAP1
PLK1 EXOSC8 SPC24 KMT5A
AURKA ATAD2 CCNA2 ⋮
TOP2A RACGAP1 CCNF

B

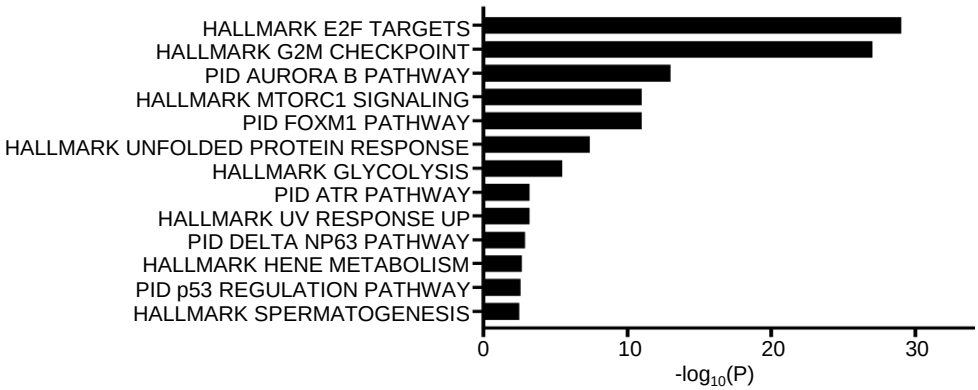
HALLMARK E2F TARGETS
HALLMARK G2M CHECKPOINT
PID AURORA B PATHWAY
HALLMARK MTORC1 SIGNALING
PID FOXM1 PATHWAY
HALLMARK UNFOLDED PROTEIN RESPONSE
HALLMARK GLYCOLYSIS
PID ATR PATHWAY
HALLMARK UV RESPONSE UP
PID DELTA NP63 PATHWAY
HALLMARK HENE METABOLISM
PID p53 REGULATION PATHWAY
HALLMARK SPERMATOGENESIS
0
10
20
30
-log10(P)

C

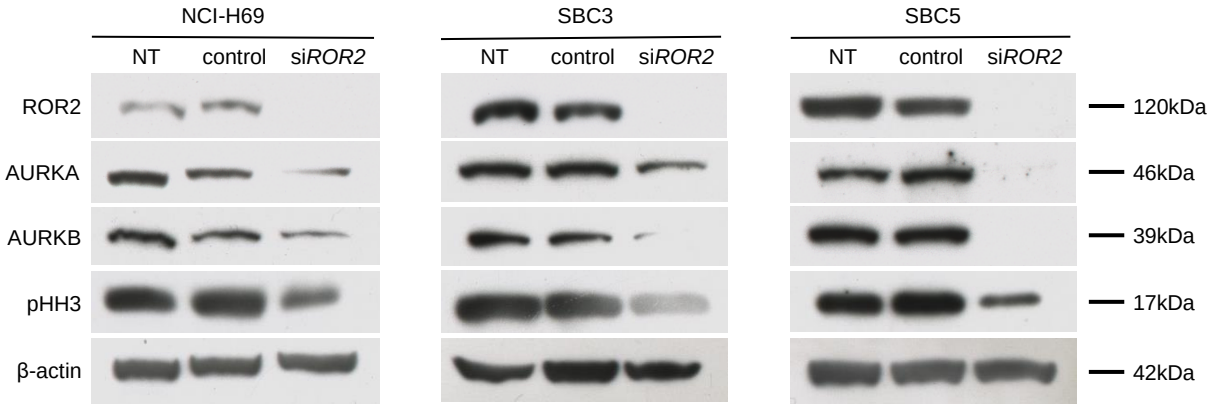
NCI-H69
SBC3
SBC5
NT
control
siROR2
ROR2
AURKA
AURKB
pHH3
β-actin
120kDa
46kDa
39kDa
17kDa
42kDa

This version of the article has been accepted for publication, after peer review (when applicable) but is not the Version of Record and does not reflect post-acceptance improvements, or any corrections. The Version of Record is available online at: https://doi.org/10.1007/s13577-022-00830-1. Use of this Accepted Version is subject to the publisher's Accepted Manuscript terms of use https://www.springernature.com/gp/open-research/policies/accepted manuscript-terms.